COPPER HEXACYANOFERRATE (II): SYNTHESIS, CHARACTERIZATION, AND CESIUM, STRONTIUM ADSORBENT APPLICATION

Nguyen Dinh Trung[a,b], Le Vu Tram Anh[a,b], Truong Dong Phuong[a], Kieu Thi Dan Thy[a], Nguyen Tran Thuy Hong[a], Ning Ping[c], Duong Thi Huong Giang[d], Ho Kim Dan[e,f *]

[a]Center for Analysis and Testing, Dalat University, Lam Dong, Vietnam
[b]Faculty of Chemistry and Environment, Dalat University, Lam Dong, Vietnam
[c]Faculty of Environmental Science and Engineering, Kunming University of Science and Technology, Kunming 650500, Yunnan, China.
[d]Lam Ha High School, Lam Dong, Vietnam
[e]Optical Materials Research Group, Science and Technology Advanced Institute, Van Lang University, Ho Chi Minh City, Vietnam
[f]Faculty of Technology, Van Lang University, Ho Chi Minh City, Vietnam
**Corresponding author: Email: trungnd@dlu.edu.vn, hokimdan@vlu.edu.vn*

Article history
Received: May 29th, 2021
Received in revised form: July 28th, 2021 | Accepted: September 29th, 2021
Available online: October 29th, 2021

Abstract

Low-cost nanoscale copper hexacyanoferrate (CuHF), a good selective adsorbent for cesium (Cs^+) removal, was prepared using the chemical co-precipitation method. Fourier transform infrared spectroscopy (FTIR), X-ray diffraction (XRD), energy-dispersive X-ray spectroscopy (EDS), and high-resolution transmission electron microscopy (HR-TEM) were conducted to determine the CuHF morphology. Copper hexacyanoferrate, $Cu_{13}[Fe(CN)_6]_{14}.(2K).10H_2O$, has a cubic structure (space group F-43m) in the range of 10–30 nm and a Brunauer-Emmett-Teller (BET) surface area of 462.42 m^2/g. The removal of Cs^+ and Sr^{2+} is dependent on pH; the maximum adsorption capacity (q_{max}) of CuHF is achieved at a pH = 6. From the Langmuir model, q_{max} = 143.95 mg/g for Cs^+ and 79.26 mg/g for Sr^{2+}, respectively. At high concentrations, Na^+, Ca^{2+}, and K^+ ions have very little effect on Cs^+ removal, and Na^+ and K^+ ions have a higher affinity for removing Sr^{2+} than Ca^{2+} at all concentrations. CuHF has a high affinity for alkaline cations in the order: $Cs^+ > K^+ > Na^+ > Ca^{2+} > Sr^{2+}$, as proposed and discussed.

Keywords: Adsorption; Cesium; Copper hexacyanoferrate; Strontium.

DOI: http://dx.doi.org/10.37569/DalatUniversity.11.4.901(2021)

Article type: (peer-reviewed) Full-length research article

1. INTRODUCTION

The nuclear power industry plays a major role in meeting the increasing energy demand caused by rapid economic development in recent years. Radionuclide elements are generated from the normal operations of nuclear power plants and accidents, such as the Three Mile Island (USA) radiation leak in 1979, the Chernobyl (Ukraine) nuclear disaster in 1986, and the Fukushima Daiichi (Japan) nuclear disaster in 2011 (Koo et al., 2014). During the operation of the Dalat nuclear reactor (Vietnam), radioactive wastewater can be generated from the purification, from cleaning the storage pool, and from water leaks. Nuclear power plant wastewater contains a large amount of soluble and insoluble radioactive compounds and other substances. The radionuclide elements have a long half-life and high fission. They are potentially harmful to humans and the environment (Ma et al., 2011; Singh et al., 2008). Several techniques capable of recovering low-metal radionuclides from high-salt-containing solutions are a challenge (Yasunari et al., 2011). The aim is how to decontaminate and reduce the volume of radioactive wastewater. After that, the concentrated wastewater undergoes a process of conditioning, storage, and disposal. The selective separation and removal of radioactive cesium ions from nuclear wastewater are challenging because of the lack of knowledge of the behavior of ultra-trace cesium and strontium ions, which compete with the high amounts of other monovalent and divalent cations in the solution. Many techniques have been developed over the past fifty years to remove radioactive Cs^+ and Sr^{2+} from wastewater. The techniques include co-precipitation, solvent extraction, ion exchange and adsorption processes, solid-phase extraction, and solvent extraction methods involving crown ethers (Todd et al., 2004; Aguila et al., 2016; Williams et al., 2015; Xu et al., 2012; Awual et al., 2014; Avramenko et al., 2011; Nilchi et al., 2011). Despite their advantages, extraction, precipitation, membrane processing, and electrodialysis methods have limitations, such as efficiency depending on solid-liquid extraction, generating aqueous and organic secondary waste, fouling and radiation damage to organic membranes, and high operation and capital costs (Rahman et al., 2011). Ion exchange/sorption methods are the most popular solution for Cs^+ removal (Işık et al., 2020; Khandaker et al., 2018; Ali et al., 2020; Vipin et al., 2016). The ion exchange/sorption methods have good chemical, thermal, and radiation stability and a wide choice of products, ensuring high selectivity for Cs^+ removal from radioactive wastewater.

Transition metal hexacyanoferrates are complex substances capable of adsorbing strontium and cesium ions from nuclear wastewater (Ali et al., 2020; Haas, 1993; Vipin et al., 2014; Kido et al., 2017; Kiener et al., 2019). The metal hexacyanoferrates have a unique structure and arrangement of electrons, so they adsorb cesium ions efficiently and selectively. These structures are favorable for the interaction and capture of small hydrated ions, such as Cs^+, K^+, NH_4^+, while the interaction and capture are hindered for metal ions with a larger hydrated radius, such as Na^+, Ca^{2+}, etc. The recovery of cesium ions from wastewater solutions can occur through precipitation processes on the surface of transition metal hexacyanoferrates or through chemical interactions with them. The cesium ions are then adsorbed by the transition metal hexacyanoferrates (Mimura et al., 1997; Haas, 1993). Both types of transition metal hexacyanoferrates analog and nanoscale particles have distinguished themselves. They are promising substances for

such applications as degradation of selected toxic PAHs (Shanker et al., 2017), catalytic activity (Ali et al., 2009), and separation of cesium (Yang et al., 2014; Ke et al., 2020).

Nanoscale copper hexacyanoferrates (CuHF) have a cubic structure in which the Cu^{2+} atom is tetrahedrally coordinated to four N atoms from CN ligands. The porous framework of copper hexacyanoferrates remains stable with a system of narrow channels and a small free volume (Avila et al., 2008). Nanoscale CuHF has been used in advanced form, as the nanochemistry of these materials has not yet been explored. However, few publications are available on cesium separation with these complexes.

The preparation and application of transitional metal hexacyanoferrates for removing strontium and cesium from solutions have been investigated over the past 50 years. Many experiments have been reported on maximum adsorption capacity, pH, or time effects; however, the most efficient adsorption procedure is not yet obvious (Ali et al., 2020; Vipin et al., 2014; Haas, 1993; Ayrault et al., 1998). The transition metal hexacyanoferrates have various compositions and structures, so their properties are also very complex. Some papers have discussed the cesium adsorption mechanism by copper hexacyanoferrate materials (Ayrault et al., 1998; Ishizaki et al., 2013), but these reports provide limited information. Some papers only mention an ion-exchange mechanism (Loos-Neskovic et al., 2004; Zong et al., 2017; Vipin et al., 2014).

The morphological differences between copper hexacyanoferrates (CuHF) lead to differences in the physical and chemical properties at the nanoscale. This study aims to introduce a cubic (Fm-3m) nanoscale copper hexacyanoferrate adsorbent prepared by a chemical co-precipitation method that is easy to perform and low in cost. The adsorbent is characterized by X-ray diffraction (XRD), Fourier transform infrared (FTIR) spectroscopy, high-resolution transmission electron microscopy (HR-TEM), energy-dispersive X-ray spectroscopy (EDS), and Brunauer-Emmett-Teller (BET) surface area. The CuHF is evaluated for its cesium and strontium adsorption behavior. The adsorption isotherm, pH, adsorption time effect, and the competition of cesium and strontium ions with other ions are studied. The results show that copper hexacyanoferrate is the most efficient in cesium and strontium recovery.

2. EXPERIMENTAL DETAILS

2.1. Materials

The high-purity reagents in this study were all prepared from analytical-grade chemicals. Double-distilled water was used to prepare the solutions for all experiments. Stock solutions of Cs^+ 1000 mg/L, Sr^{2+} 1000 mg/L, $K_4[Fe(CN)_6].3H_2O$, and $CuSO_4.5H_2O$ (Merck, Germany) were used. Stock solutions (500 mg/L) of potassium (K^+), sodium (Na^+), and calcium (Ca^{2+}) ions were prepared separately from sodium chloride (NaCl), potassium chloride (KCl) and calcium chloride ($CaCl_2$). All solutions were used as competing ions in the Cs^+ and Sr^{2+} adsorption experiments.

Cesium (Cs^+) and strontium (Sr^{2+}) working solutions were freshly prepared by diluting CsCl and $SrCl_2.6H_2O$ with double-distilled water. HNO_3 (0.1–0.5 N) and NaOH (0.1–0.5 N) were used to adjust the cesium solution pH as necessary. The cesium and strontium in the solutions were analyzed before and after the adsorption experiments with a Shimadzu AA-7000 atomic absorption spectrometer (Japan) and a Bruker S2 Picofox total reflection X-ray fluorescence spectrometer (Germany). For safety, stable isotopes of cesium and strontium salts were used in the research.

2.2. Methods

2.2.1. Preparation of CuHF adsorbent

The CuHF adsorbent was prepared according to the following procedure. $CuSO_4.5H_2O$ was dissolved with vigorous stirring in 750 ml of double-distilled water to obtain concentrations of 0.15 M. The reactor beaker was placed in an ultrasonic bath. The beaker was equipped with a drop funnel containing 250 mL of $K_4[Fe(CN)_6]$ (0.05 M). The $K_4[Fe(CN)_6]$ solution was slowly dropped into the reactor beaker, which contained a continuously stirred copper sulfate solution. The temperature was maintained at 40 ºC. The adsorbent synthesis process was carried out in an ultrasonic bath (Elma S300H, 1500 W-50 Hz). After 4 hours of reaction, the chocolate-colored precipitate was collected and rinsed five times with double-distilled water, centrifuged (Universal 320-Germany) at 10,000 rpm, and dried at 60 ºC for 24 h. After drying, the material was finely ground to prepare for further experiments.

2.2.2. Characterization of CuHF adsorbent

The adsorbent was characterized with XRD, FTIR spectroscopy, HR-TEM, EDS, and BET. All experimental measurements were performed at ambient air temperature.

2.2.3. Batch sorption tests

To determine the adsorption capacity of cesium by CuHF under the given conditions, we weighed exactly 0.1 g of copper hexacyanoferrate and placed it in a 250 mL Erlenmeyer flask that contained 100 mL of a cesium solution. Cesium solution concentrations of 75, 100, 120, 145, 170, 200, 230, and 250 mg/L were used. A similar procedure was used for determining the adsorption capacity of strontium by CuHF, except that 1 g of copper hexacyanoferrate was used, and the strontium solution concentrations were 40, 100, 150, 200, 250, 300, 400, 450, and 550 mg/L.

The pH of the solution was not adjusted during the adsorption process. The flask was shaken with an IKA HS 260 basic shaker (USA) at 270 rpm for 24 h. All batch experiment processes were carried out at ambient air temperature (25 °C). The initial pH of the adsorption experiment solution was adjusted to a defined value with 0.01 N HNO_3 or NaOH and maintained at a designated pH value. After 24 h of the reaction, all samples were centrifuged with a Universal 320 centrifuge (Germany) at 10,000 rpm for 5 minutes and filtered through a 0.22-µm membrane filter. The filtrate was analyzed for

cesium and strontium. All adsorption experiments for evaluating isotherms, pH, and contact time effects followed batch sorption test.

The cesium and strontium adsorption capacities of copper hexacyanoferrate were calculated by the change in the cesium and strontium concentrations before and after the adsorption process. The adsorption capacities of cesium and strontium by the adsorbent are calculated from the following expression:

$$q_e = \frac{\mathrm{V}(C_i - C_e)}{\mathrm{B}} \quad (1)$$

where q_e is the adsorption capacity of the adsorbent (in mg/g of adsorbent), C_i and C_e are the cesium or strontium concentrations (mg/L) before and after the adsorption process, respectively, B is the mass (g) of the adsorbent, and V is the solution volume (L).

The Langmuir adsorption equation is

$$q_e = \frac{\mathrm{Q_m\ bC_e}}{1+\mathrm{bC_e}} \quad (2)$$

where q_e is the amount of cesium or strontium ions adsorbed by the materials (mg/g), Q_m is the maximum adsorption capacity of cesium or strontium ions, C_e is the concentration at a point of adsorption (mg/L), and b is the rate constant between adsorption and desorption.

The Freunlich adsorption equation is

$$q_\mathrm{e} = \mathrm{K}_f \mathrm{C}_\mathrm{e}^{1/\mathrm{n}} \quad (3)$$

where K_f and n are the adsorption constants on reaching equilibrium.

2.2.4. Studies of Adsorption

The effect of pH on cesium and strontium adsorption was examined in a series of batch sorption experiments that used the same initial concentrations of Cs^+ (140 mg/L) and Sr^{2+} (150 mg/L). The pH was maintained at values of 2.0, 3.0, 4.0, 5.0, 6.0, 7.0, 8.0, and 9.0.

All experiments on cesium and strontium adsorption isotherms were conducted at 25 ºC and pH = 6 following the batch adsorption procedure. A series of different initial concentrations of Cs^+ solutions (75–250 mg/L) and Sr^{2+} solutions (40–550 mg/L) were used for evaluating the isothermal parameters of cesium and strontium adsorption.

The effects of time on cesium and strontium adsorption were examined in a series of batch sorption experiments that used the same initial Cs^+ concentration (10 mg/L) and Sr^{2+} concentration (40 mg/L) while varying time from 0 to 25 hours. The interference of Ca^{2+}, K^+, and Na^+ on the Cs^+ or Sr^{2+}adsorption was evaluated in batch

experiments. The experimental method was similar to the batch adsorption method described above. The solutions for these competing adsorption experiments were prepared with the addition of Ca^{2+}, K^{+}, and Na^{+} solutions into the Cs^{+} or Sr^{2+} solution. The concentrations of the Ca^{2+}, K^{+}, and Na^{+} competing all cations ranged from 0 to 120 mg/L.

3. RESULTS AND DISCUSSION

3.1. Characterization of CuHF adsorbent

Figure 1 shows the FTIR spectrum of the CuHF. The spectrum featured a ν(CN) band of CuHF at 2099.59 cm^{-1}. The CuHF FTIR spectrum is composed of three vibrations within the octahedral unit, $[Fe(CN)6]^{4-}$: ν(CN), δ(Fe-CN), and ν(Fe-C). At the same time, the motions from crystal water, ν(OH), and δ(HOH) are present (Nakamoto, 1986). This relatively high frequency for the ν(CN) band in a ferrocyanide suggests a tetrahedral $[Fe(CN)6]^{4-}$ coordination for the copper atom. When the Cu atom is octahedrally coordinated to N ends of CN groups, this vibration is an observed band below 2095 cm^{-1}. Similar evidence obtained from the δ(Fe-CN) and ν(Fe-C) frequencies was observed in the bands at 590.92 cm^{-1} and 472.71 cm^{-1}, respectively.

For this compound, a δ(HOH) narrowband at 1623.14 cm^{-1} was observed. In the ν(OH) region, two absorption bands at 3609.12 cm^{-1} and 3452.00 cm^{-1} appear, ascribed to symmetric and asymmetric OH stretching, respectively, of coordinated water. This result indicates the existence of one type of crystal binding to water molecules: $CuHF.xH_2O$. The FTIR spectrum of this study is also consistent with the research results of Avila et al. (2008).

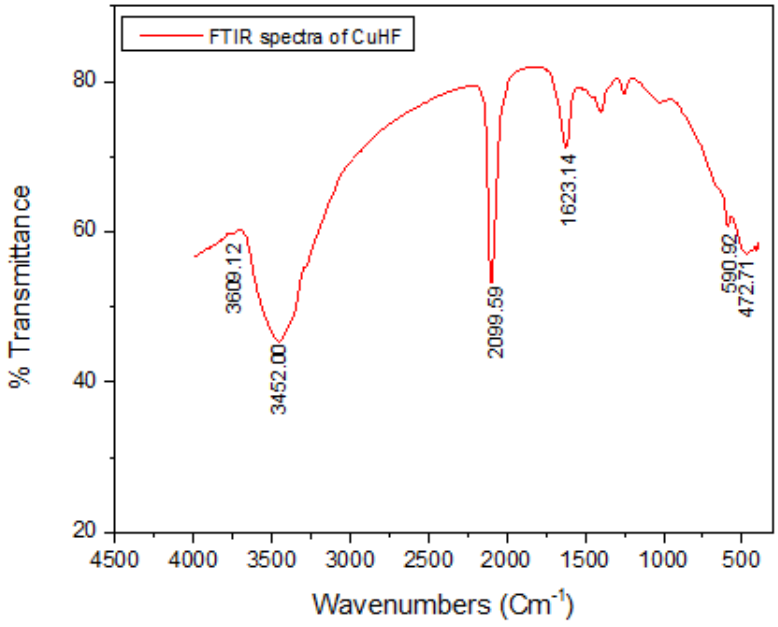

Figure 1. FTIR spectrum of CuHF

The elemental composition of the complex substance was examined using transmission electron microscopy coupled with energy-dispersive X-ray spectroscopy (EDS). The EDS spectrum of $CuHF.xH_2O$ is shown in Figure 2.

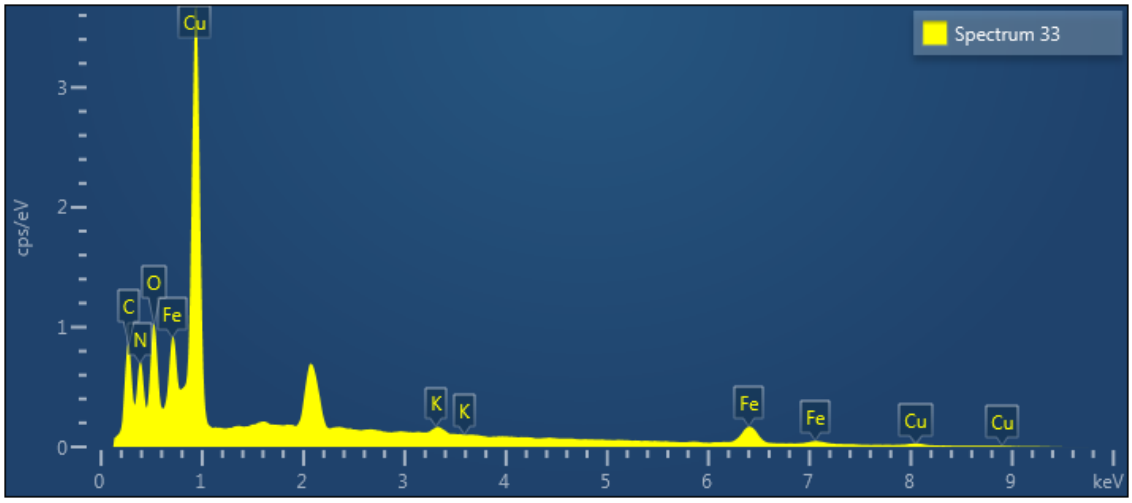

Figure 2. EDS spectrum of CuHF

Table 1. Elemental composition of the complex substance

Element	Line Type	Weight (%)	Atomic (%)
Cu	L series	22.74	7.11
Fe	L series	18.71	6.64
C	K series	24.05	39.81
N	K series	28.06	39.81
O	K series	4.58	5.69
K	K series	1.86	0.95

The atomic percentages of different elements of the complex substance are given in Table 1, from which it can be deduced that the molecular formula of the copper hexacyanoferrate was $Cu_{13}[Fe(CN)_6]_{14}.(2K).10H_2O$. CuHF exhibits a great variety of compositions and structures. Several compositions may be observed with the same transition metal, depending on the preparation method (Kiener et al., 2019).

Previous papers have reported on synthesized copper hexacyanoferrate with the formula $K_{1.97}Cu^{II}_{1.00}Fe(CN)_6$ (Loos-Neskovic et al., 2004), $K_{2/3}Cu[Fe(CN)_6]_{2/3}\cdot zH2O$ (Takahashi et al., 2016), and $K_2CuFe(CN)_6$ (Wang et al., 2009). In a chemical formula, the indices must be integers such as 1, 2, 3. Expressing the chemical formula as $K_{1.97}Cu^{II}_{1.00}Fe(CN)_6$ causes misunderstanding. If the complex molecules contain potassium in the $K_2CuFe(CN)_6$ framework, this component may be water-soluble (Vincent et al., 2015).

The adsorbent was prepared according to the following chemical equations:

$$2CuSO_4 \text{ (redundant)} + K_4[Fe(CN)_6] \rightarrow Cu_2[Fe(CN)_6] + 2K_2SO_4 \quad (4)$$

$$CuSO_4 + K_4[Fe(CN)_6] \text{ (redundant)} \rightarrow K_2Cu[Fe(CN)_6] + K_2SO_4 \quad (5)$$

The $K_2Cu[Fe(CN)_6]$ dissolves in the solution (Vincent et al., 2015), so it was removed after the chocolate-colored precipitate was rinsed with double-distilled water five times. Thus, the K^+ ions in the adsorbent (Figure 2) may be the ions that were adsorbed by the adsorbent that had just been prepared.

The morphology of the complex substance (CuHF) is shown in Figure 3. The bulk structures of the adsorbents can be seen in the HR-TEM image, and they have precise geometric shapes. The TEM micrographs of the complex substance show a zeolitic structure in the range of 10–30 nm.

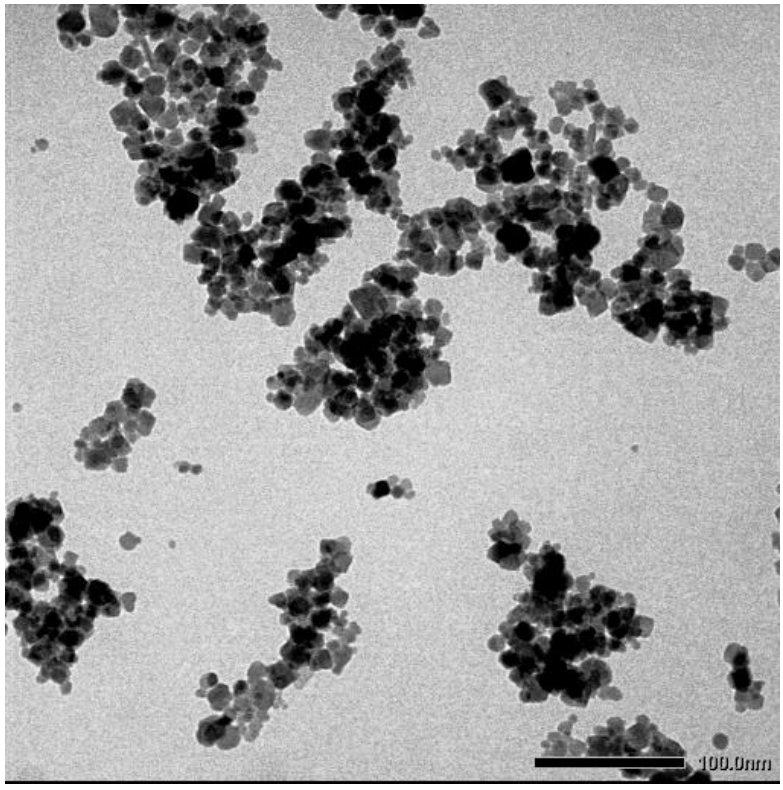

Figure 3(a). HR-TEM image of CuHF

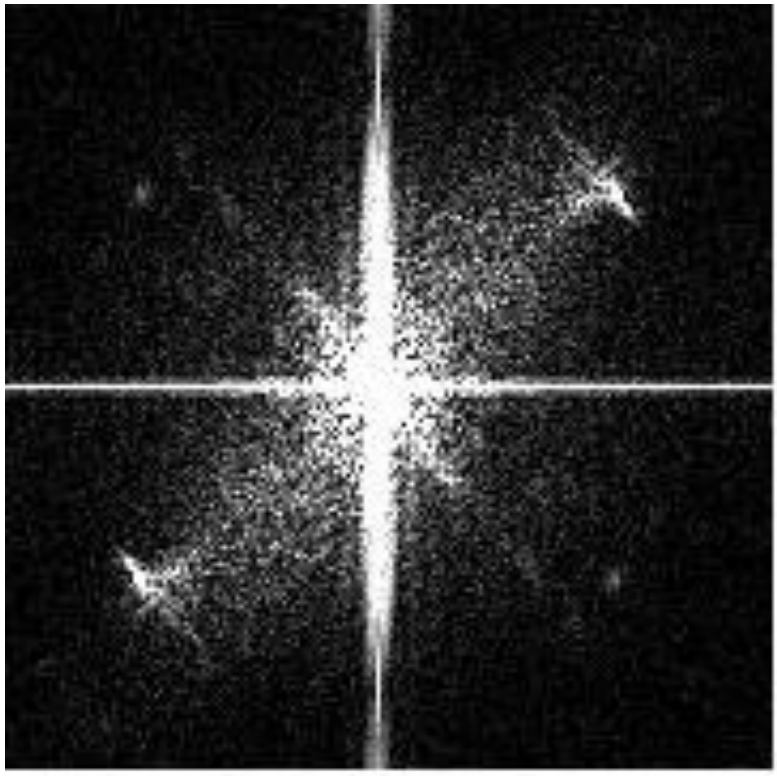

Figure 3(b). HR-TEM image of one unit cell of CuHF

The evidence from the XRD data was analyzed by FullProf Suite software with standard 101038.cif (Murray-Rust, 2021) to identify the crystal structure of CuHF that had just been prepared. The solid red circles are the XRD diagram of $Cu_2Fe(CN)_6$, and the blue line is the standard diagram.

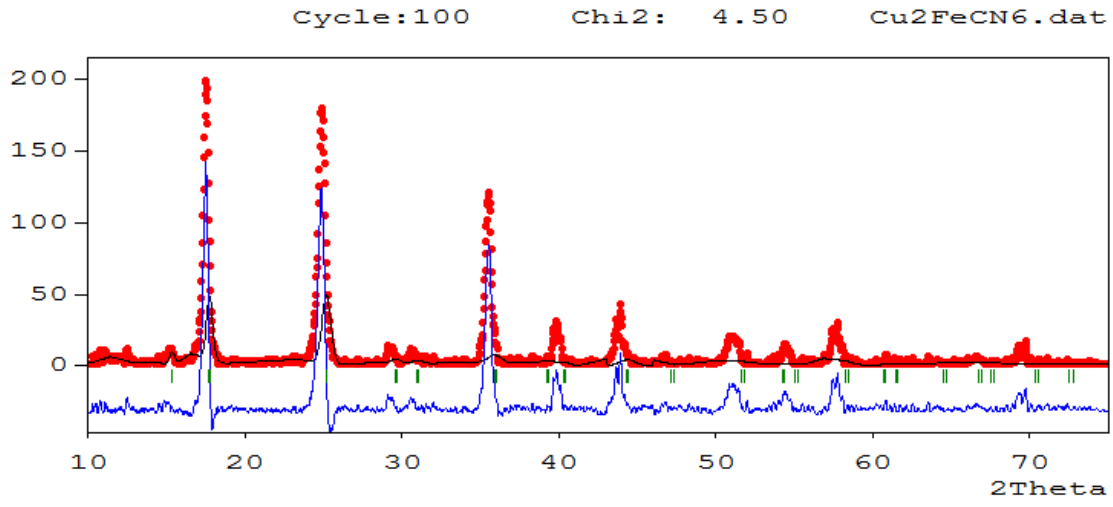

Figure 4. XRD diagram of CuHF compared to the standard

Note: $Cu_2Fe(CN)_6$ is shown as solid red circles; the standard is shown as a blue line.

The Miller indices [h, k, l] of the CuHF Bravais lattice and crystal system were calculated by Rietveld refinement using FullProf Suite software. The results indicate that the sample has the same main copper hexacyanoferrate peak as the standard. The main cubic crystal has Miller indices d[h,k,l]:

$d[1,1,1] = \frac{a}{\sqrt{3}} = 5.01$, $d[2,0,0] = \frac{a}{2} = 3.04$, and $d[2,2,0] = \frac{a}{2\sqrt{2}} = 3.01$ … The main cubic crystal is combined with eight subcubics (Sun et al., 2020).

The morphology of copper hexacyanoferrate was further characterized by high-resolution transmission electron microscopy (HR-TEM). The picture of one unit cell (in Figure 3b) and the elemental composition of the complex substance (Table 1) are enough to confirm the cubic structure of CuHF (space group F-43m). The crystal structure of one unit cell drawn with VESTA software is presented in Figure 5.

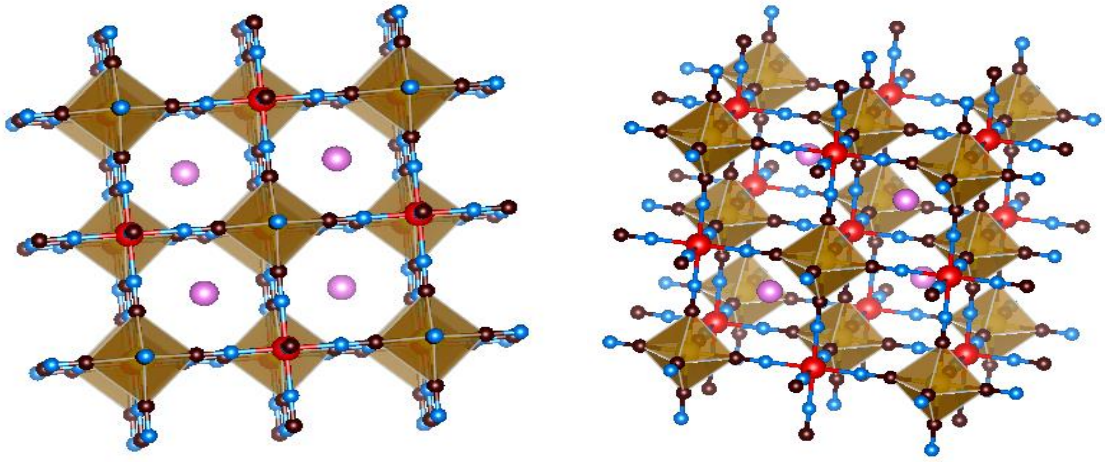

Figure 5. A unit cell of $Cu_{13}[Fe(CN)_6]_{14}.(2K).10H_2O$

Note: blue (N), black (C), red (Cu), yellow (Fe), pink (H_2O or Cu^{2+}, K^+).

Table 2. The physicochemical characteristics of CuHF

BET surface area	462.42 m^2/g
Pore volume	0.07 cm^3/g
D-H adsorption average pore width	3.12 nm

Copper hexacyanoferrate has a cubic zeolitic structure in the range of 10–30 nm with cavities that can host K^+ ions and water molecules (Loos-Neskovic et al., 2004). CuHF is suitable to adsorb cesium; it can be prepared repeatedly and maintains constant composition. The BET surface area is 462.42 m^2/g (Table 2). The complex substance is an adsorbent for further experiments.

3.2. The effect of pH on adsorption

The adsorption of Cs^+ and Sr^{2+} onto CuHF as a function of the initial concentration pH is shown in Figure 6. The removal of Cs^+ and Sr^{2+} was dependent on pH, with the most significant adsorption occurring under near-neutral pH.

For cesium (Figure 6a), the maximum adsorption capacity is at pH = 6. This result agrees with that of the Loos-Neskovic group (pH 5–8), while the report of Clarke and Wai shows the selective removal of cesium by CuHF from neutral to acidic solutions (Clarke & Wai, 1998). For strontium (Figure 6b), the maximum adsorption capacities of CuHF range in pH from 4 to 9. This result agrees with that of the Vipin group (pH 4–9) (Vipin et al., 2014). Therefore, we chose to do all tests at pH = 6 in these experiments.

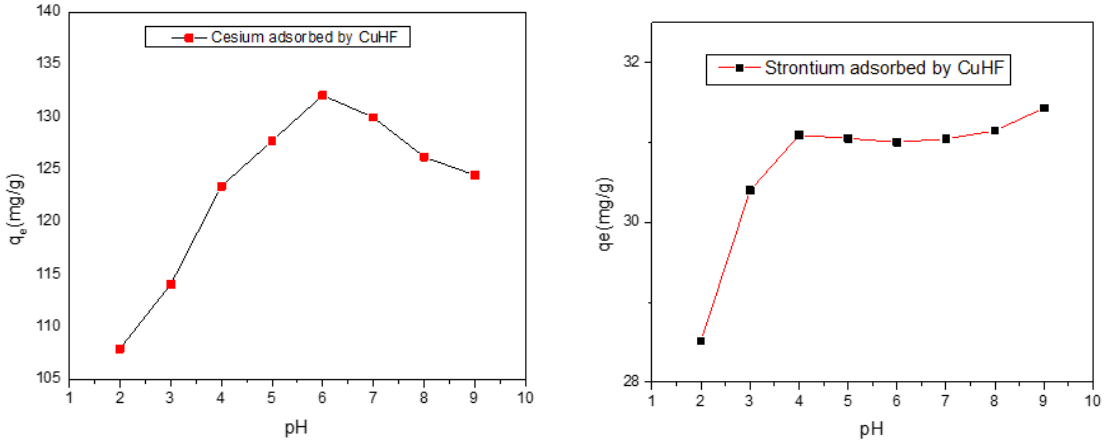

(a) (b)

Figure 6. Cesium and strontium ion adsorption onto CuHF at various initial pH

Note: (a) Cesium ion adsorption onto CuHF (1 gL^{-1}); (b) Strontium ion adsorption onto CuHF (10 gL^{-1}).

3.3. The adsorption isotherm effect

For cesium (Table 3), the amount of Cs^+ removed increases significantly with an increase in the initial Cs^+ concentration because of a stronger dynamic of mass transfer at higher concentrations (Figure 7). However, the adsorption slows slightly when the maximum adsorption capacity is reached above an initial concentration of 170 mg/L Cs^+, after which the Cs^+ adsorption rate decreases as the initial Cs^+ concentration increases. When the concentration of Cs^+ is 200 mg/L, the amount of Cs^+ adsorption is 142.21 mg/g. When the concentration of Cs^+ is increased to 250 mg/L, the adsorption capacity of Cs^+ ions by copper hexacyanoferrate increases slightly. These results are likely due to the higher Cs^+ concentration, more saturated adsorption sites, and the observed reduced removal efficiency. The highest adsorption capacity of Cs^+ ions by CuHF was found to be 144.17 mg/g.

For strontium (Table 4), the adsorption process occurs strongly when the initial concentration of strontium in solution is high. When the concentration of Sr^{2+} is 400 mg/L, the amount of Sr^{2+} adsorption is 39.93 mg/g. When the concentration of Sr^{2+} is increased to 550 mg/L, the adsorption capacity of Sr^{2+} ions by CuHF increases slightly.

Table 3. Cesium ion adsorption onto CuHF (1 gL^{-1}) at various initial cesium concentrations

Cesium concentration C_i (mg/L) before adsorption	Cesium concentration C_e (mg/L) after adsorption	Mass B of adsorbent (g)	Solution volume V(L)	Adsorption capacity of adsorbent q_e(mg/g)	Adsorption capacity of adsorbent q_e(mEq/g)
75	1.05	0.10	0.10	73.95	0.56
100	4.29	0.10	0.10	95.71	0.72
120	5.89	0.10	0.10	114.11	0.86
145	10.48	0.10	0.10	134.52	1.01
170	32.17	0.10	0.10	137.83	1.04
200	67.79	0.10	0.10	142.21	1.07
230	86.67	0.10	0.10	143.33	1.08
250	105.83	0.10	0.10	144.17	1.08

Table 4. Strontium ion adsorption onto CuHF (10 gL^{-1}) at various initial strontium concentrations

Strontium concentration C_i (mg/L) before adsorption	Strontium concentration C_e (mg/L) after adsorption	Mass B of adsorbent (g)	Solution volume V(L)	Adsorption capacity of adsorbent q_e(mg/g)	Adsorption capacity of adsorbent q_e(mEq/g)
41.46	0.15	1	0.10	4.13	0.09
107.39	0.59	1	0.10	10.68	0.25
147.72	0.92	1	0.10	14.68	0.34
189.57	1.24	1	0.10	18.83	0.43
250.59	1.95	1	0.10	24.86	0.57
313.49	3.11	1	0.10	31.04	0.72
403.14	3.85	1	0.10	39.93	0.92
474.11	6.71	1	0.10	46.74	1.08
561.76	8.81	1	0.10	55.29	1.28

All experiments were conducted at 25 ºC and pH = 6 by following the batch adsorption procedure. The amounts of Cs^+ and Sr^{2+} uptake by CuHF are shown in Figures 7 and 8. The Langmuir and Freundlich isotherm parameters for the adsorbed Cs^+ and Sr^{2+} ions are given in Table 5.

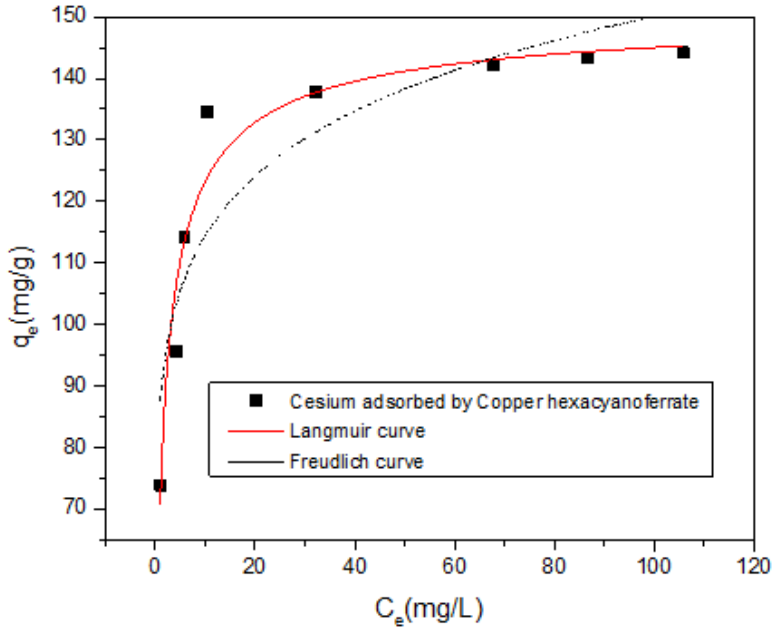

Figure 7. Langmuir and Freundlich isotherms for the adsorption of Cs^+ on CuHF

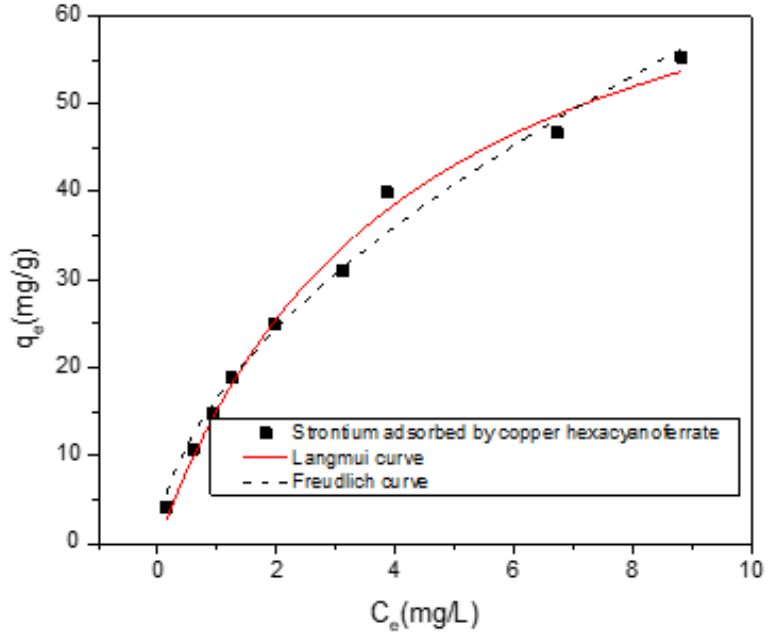

Figure 8. Langmuir and Freundlich isotherms for the adsorption of Sr^{2+} on CuHF

Table 5. Langmuir and Freundlich isotherm parameters for Cs^+ and Sr^{2+} adsorption

Langmuir model			
	Q_m (mg/g)	b	R^2
Cs^+	143.95	0.76	0.91
Freundlich model			
	K_f (mg/g)	1/n	R^2
Cs^+	87.14	0.12	0.81
Langmuir model			
	Q_m (mg/g)	b	R^2
Sr^{2+}	79.26	0.24	0.98
Freundlich model			
	K_F (mg/g)	1/n	R^2
Sr^{2+}	16.57	0.56	0.98

The correlation coefficients (R^2) of the Langmuir isotherms were 0.91 and 0.98, while those of the Freundlich isotherm were 0.81 and 0.98 for cesium and strontium adsorbed by CuHF, respectively. The Langmuir model was conformable to describe the adsorption process of Cs^+ and Sr^{2+} by CuHF because the regression correlation coefficients were high. The maximum cesium adsorption capacity calculated according to the Langmuir model Q_{max} = 143.95 mg/g was equivalent to the experimental value of 143.33 mg/g. In comparison, the strontium adsorbing capacity calculated according to the Langmuir model was higher than the experiment value.

The maximum adsorption capacities of various adsorbing materials for cesium and strontium are shown in Table 6. The copper hexacyanoferrate used in this study has a high uptake capacity for cesium compared to several other materials.

Table 6. The Cs^+ and Sr^{2+} adsorption capacities of various adsorbent materials

Adsorbent	pH	Maximum cesium adsorption capacity (mg g^{-1})	Maximum strontium adsorption capacity (mg g^{-1})	Reference
Copper hexacyanoferrate	6.0	143.95	79.26	This study
MIL-101-SO3H	6.0	36.47	-	Aguila et al., 2016
Zeolite	2-10	102	96.15	Vipin et al., 2016
Zeolite + MWCNT	2-10	113.6	107.5	Vipin et al., 2016
Zeolite A	2-8	207.47	303	El-Kamash et al., 2008
AC-PBNP	6.8	36.1	9.26	Ali et al., 2020

Table 6. The Cs^+ and Sr^{2+} adsorption capacities of various adsorbent materials (cont.)

Adsorbent	pH	Maximum cesium adsorption capacity (mg g^{-1})	Maximum strontium adsorption capacity (mg g^{-1})	Reference
Nanozeolite composite	7	208.38	97.08	Faghihian et al., 2013
Microzeolite composite	7	160.01	78.90	Faghihian et al., 2013

3.4. The adsorption time effect

Adsorption kinetics is one of the critical factors that need to be considered for determining the efficiency of the adsorption process. Hence, in this study, the kinetics of cesium and strontium adsorption was analyzed to understand the adsorption behavior of CuHF. Figure 9 shows the Cs^+ adsorption data by this adsorbent at pH = 6 for different time intervals. The adsorption was found to be time-dependent. The adsorption of Cs^+ was rapid for the first 10 minutes, at which the removal rate reached 62%. The adsorption equilibrium was approached after 18 minutes, and the removal of cesium ions from the experiment solution was 97.03%.

The Hwang group found that the cesium uptake by CuHF reached equilibrium within 10 minutes (Hwang et al., 2017). Parajuli et al. (2016) suggested that the optimal pH is within the range of 4 to 8 and that the time needed to reach equilibrium is under 2 hours.

Strontium adsorption was also found to be time-dependent (Figure 10). The adsorption equilibrium was reached after 18 hours, and the strontium ion removal from the experiment solution was 71.29%.

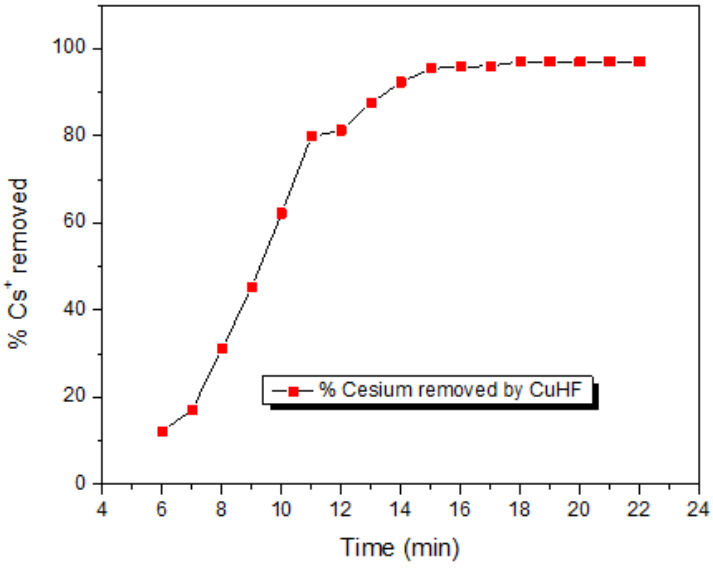

Figure 9. Sorption time of Cs^+ ions by CuHF

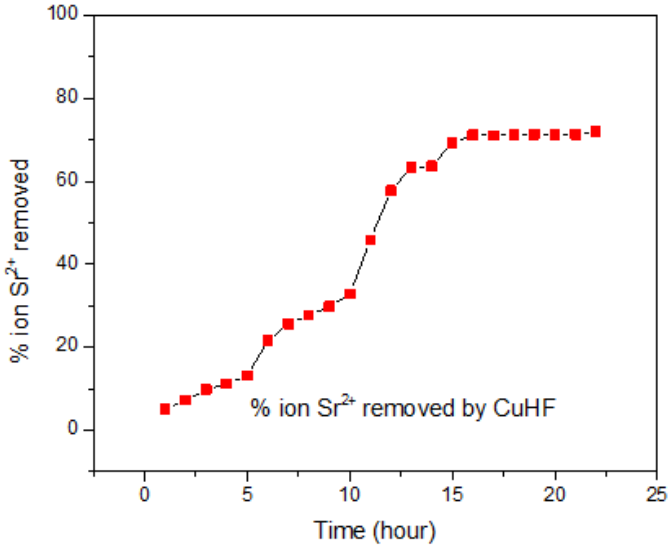

Figure 10. Sorption time of Sr^{2+} ions by CuHF

3.5. Cesium and strontium ion adsorption in competition with other constituent ions

Several components may exist in radioactive wastewater that compete with cesium and strontium for adsorption sites or interact with themselves. Ca^{2+}, K^{+}, and Na^{+} ions were selected to test the effect of co-existing constituents.

Figure 11 shows that the co-existing ions, Ca^{2+}, Na^{+}, and K^{+}, had little effect on cesium removal, and then only if they were in high concentration (over ten times higher than the cesium concentration). The effects of increased Ca^{2+} concentration levels at pH = 6 are illustrated in Figure 11 and show little adsorption competition. In high concentrations, calcium and potassium probably precipitated on the adsorbent surface and interfered with the Cs^{+} adsorption process. Na^{+} had little effect on the adsorbent performance in removing cesium.

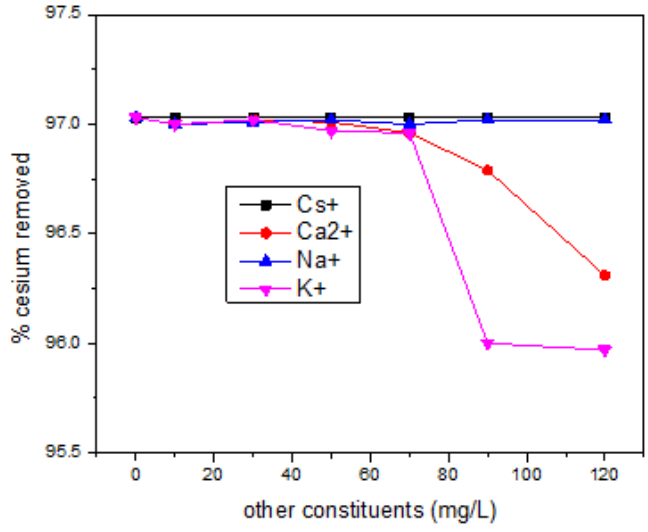

Figure 11. Constituent effect on the adsorption of Cs^{+} by CuHF

Figure 12 shows that the presence of co-existing ions, Ca^{2+}, Na^{+}, and K^{+}, significantly decreased the strontium removal from 70 % to 0% compared with the base. In all concentrations, the monovalent ions have a higher affinity for CuHF than the divalent ions in the adsorption process. Calcium ions showed a lower effect on strontium adsorption than potassium ions.

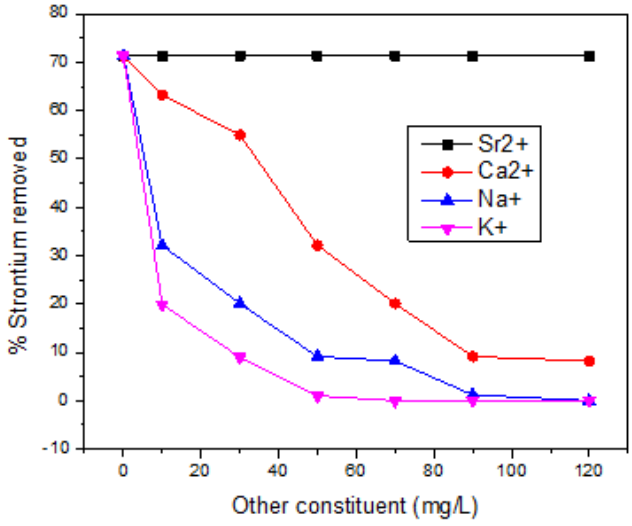

Figure 12. Constituent effect on the adsorption of Sr^{2+} by CuHF

When studying the effects of other elements in the solution, the Gad group reported that sodium and calcium affect the adsorption of cesium by copper hexacyanoferrate (Gad et al., 2016). This study compares with the Gad group's results; the effect occurs only when the competing ion concentration is very high compared to the original cesium concentration. In the presence of Ca^{2+} and K^{+} ions, the total amount of cesium adsorbed decreased by 3% compared to the base, but when the Na^{+} ion is present in the solution, the amount of cesium adsorbed is not significantly reduced.

The above finding can be explained in terms of ionic radii. The radius of hydrated K^{+} $M^{+}(H_2O)_n$ (3.31 Å) is close to that of hydrated cesium (3.29 Å); therefore, the K^{+} ions can compete with the adsorption of cesium ions. In contrast, the radii of hydrated Ca^{2+} (4.12 Å) and Na^{+} (3.58 Å) are larger than that of the hydrated cesium ion; therefore, the Ca^{2+} and Na^{+} ions cannot compete with the cesium ion adsorption.

From the research results discussed above, the CuHF has a high affinity for alkaline cations in the order: $Cs^{+} > K^{+} > Na^{+} > Ca^{2+} > Sr^{2+}$.

4. CONCLUSIONS

A low-cost nanoscale copper hexacyanoferrate adsorbent for cesium **(**Cs^{+}) removal was prepared using the chemical co-precipitation method. The adsorbent, $Cu_{13}[Fe(CN)_6]_{14}.(2K).10H_2O$, has a cubic structure with the space group F-43m in the range of 10–30 nm and a BET surface area of 462.42 m^2/g. The removal of Cs^{+} and Sr^{2+}

is dependent on pH. The maximum adsorption capacity of the material is reached at pH = 6. The Langmuir model was conformable to describe the adsorption process of Cs^+ and Sr^{2+} by CuHF due to the high regression correlation coefficient. The maximum adsorption capacities calculated with the Langmuir model are q_{max} = 143.95 mg/g and 79.26 mg/g for Cs^+ and Sr^{2+}, respectively. The adsorption of Cs^+ was rapid; after 18 minutes, 97.03% of the Cs^+ was removed from the experiment solution. In contrast, the adsorption of Sr^{2+} was slow; it took up to 18 hours for 71.29% of the strontium content to be removed from the solution.

The Na^+, Ca^{2+}, and K^+ ions in the solution affected the removal of Cs^+ only slightly, and only when present in high concentrations.

The monovalent ions have a higher affinity for the strontium ion than do the divalent ions in all concentrations. These results indicated that nanoscale CuHF is an attractive adsorbent for removing Cs^+ from aqueous radioactive wastewater.

5. ACKNOWLEDGMENTS

This study was supported by the Ministry of Education & Training, Vietnam (No. B2020 DLA 01).

REFERENCES

Aguila, B., Banerjee, D., Nie, Z., Shin, Y., Ma, S., & Thallapally, P. K. (2016). Selective removal of cesium and strontium using porous frameworks from high level nuclear waste. *Chemical Communications*, *52*(35), 5940-5942.

Ali, M. M. S., Sami, N. M., & El-Sayed, A. A. (2020). Removal of Cs^+, Sr^{2+} and Co^{2+} by activated charcoal modified with Prussian blue nanoparticle (PBNP) from aqueous media: Kinetics and equilibrium studies. *Journal of Radioanalytical and Nuclear Chemistry*, *324*(11), 189-201.

Ali, S. R., Bansal, V. K., Khan, A. A., Jain, S. K., & Ansari, M. A. (2009). Growth of zinc hexacyanoferrate nanocubes and their potential as heterogeneous catalyst for solvent-free oxidation of benzyl alcohol. *Journal of Molecular Catalysis A: Chemical*, *303*(1-2), 60-64.

Avila, M., Reguera, L., Rodríguez-Hernández, J., Balmaseda, J., & Reguera, E. (2008). Porous framework of $T_2[Fe(CN)_6]\bullet xH_2O$ with T=Co, Ni, Cu, Zn, and H_2 storage. *Journal of Solid State Chemistry*, *181*(11), 2899-2907.

Avramenko, V., Bratskaya, S., Zheleznov, V., Sheveleva, I., Voitenko, O., & Sergienko, V. (2011). Colloid stable sorbents for cesium removal: Preparation and application of latex particles functionalized with transition metals ferrocyanides. *Journal of Hazardous Materials*, *186*(2-3), 1343-1350.

Awual, M. R., Yaita, T., Taguchi, T., Shiwaku, H., Suzuki, S., & Okamoto, Y. (2014). Selective cesium removal from radioactive liquid waste by crown ether

immobilized new class conjugate adsorbent. *Journal of Hazardous Materials, 278*, 227-235.

Ayrault, S., Jimenez, B., Garnier, E., Fedoroff, M., Jones, D. J., & Loos-Neskovic, C. (1998). Sorption mechanisms of cesium on $Cu^{II}_2Fe^{II}(CN)_6$ and $Cu^{II}_3[Fe^{III}(CN)_6]_2$ hexacyanoferrates and their relation to the crystalline structure. *Journal of Solid State Chemistry*, *141*(2), 475-485.

Clarke, T. D., & Wai, C. M. (1998). Selective removal of cesium from acid solutions with immobilized copper ferrocyanide. *Analytical Chemistry*, *70*(17), 3708-3711.

El-Kamash, A. M. (2008). Evaluation of zeolite A for the sorptive removal of Cs+ and Sr2+ ions from aqueous solutions using batch and fixed bed column operations. *Journal of Hazardous Materials, 151*(2-3), 432-445.

Faghihian, H., Iravani, M., Moayed, M., & Ghannadi-Maragheh, M. (2013). Preparation of a novel PAN–zeolite nanocomposite for removal of Cs^+ and Sr^{2+} from aqueous solutions: Kinetic, equilibrium, and thermodynamic studies. *Chemical Engineering Journal, 222*, 41-48.

Gad, H. M. H., Elsanafeny, H. A., Ali, M. M. S., Lasheen, Y. F., Abdelwahed, M. G. (2016). Factors affecting the sorption behavior of Cs^+ and Sr^{2+} using biosorbent material. *Russian Journal of Applied Chemistry, 89*, 988-999.

Haas, P. A. (1993). A review of information on ferrocyanide solids for removal of cesium from solutions. *Separation Science and Technology, 28*(17-18), 2479-2506.

Hwang, K. S., Park, C. W., Lee, K.-W., Park, S.-J., & Yang, H.-M. (2017). Highly efficient removal of radioactive cesium by sodium-copper hexacyanoferrate-modified magnetic nanoparticles. *Colloids and Surfaces A: Physicochemical and Engineering Aspects*, *516*, 375-382.

Ishizaki, M., Akiba, S., Ohtani, A., Hoshi, Y., Ono, K., Matsuba, M., Togashi, T., Kananizuka, K., Sakamoto, M., Takahashi, A., Kawamoto, T., Tanaka, H., Watanabe, M., Arisaka, M., Nankawa, T., & Kurihara, M. (2013). Proton-exchange mechanism of specific Cs^+ adsorption via lattice defect sites of Prussian blue filled with coordination and crystallization water molecules. *Dalton Transactions, 42*(45), 16049-16055.

Işık, B., Kurtoğlu, A. E., Gürdağ, G., & Keçeli, G. (2020). Radioactive cesium ion removal from wastewater using polymer metal oxide composites. *Journal of Hazardous Materials*, *403*, 123652.

Ke, Y., Li, Y., Zhu, L., Zhou, Y., & Liu, D. (2020). Rapid enrichment of cesium ions in aqueous solution by copper ferrocyanide powder. *SN Applied Sciences*, *2*(4), 522.

Khandaker, S., Toyohara, Y., Kamida, S., & Kuba, T. (2018). Adsorptive removal of cesium from aqueous solution using oxidized bamboo charcoal. *Water Resources and Industry*, *19*, 35-46.

Kido, G., Takasaki, M., Minami, K., Tanaka, H., Ogawa, H., Kawamoto, T., & Yoshino, K. (2017). Analysis of Cs-adsorption behavior using a column filled with microcapsule beads of potassium copper hexacyanoferrate. *Journal of Nuclear Science and Technology, 54*(11), 1157-1162.

Kiener, J., Limousy, L., Jeguirim, M., Le Meins, J.-M., Hajjar-Garreau, S., Bigoin, G., & Ghimbeu, C. M. (2019). Activated carbon/transition metal (Ni, In, Cu) hexacyanoferrate nanocomposites for cesium adsorption. *Materials, 12*(8), 1253.

Koo, Y.-H., Yang, Y.-S., & Song, K.-W. (2014). Radioactivity release from the Fukushima accident and its consequences: A review. *Progress in Nuclear Energy, 74*, 61-70.

Loos-Neskovic, C., Ayrault, S., Badillo, V., Jimenez, B., Garnier, E., Fedoroff, M., Jones, D. J., & Merinov, B. (2004). Structure of copper-potassium hexacyanoferrate (II) and sorption mechanisms of cesium. *Journal of Solid State Chemistry, 177*(6), 1817-1828.

Ma, B., Oh, S., Shin, W. S., & Choi, S.-J. (2011). Removal of Co^{2+}, Sr^{2+} and Cs^{+} from aqueous solution by phosphate-modified montmorillonite (PMM). *Desalination, 276*(1-3), 336-346.

Mimura, H., Lehto, J., & Harjula, R. (1997). Selective removal of cesium from simulated high-level liquid wastes by insoluble ferrocyanides. *Journal of Nuclear Science and Technology, 34*(6), 607-609.

Murray-Rust, P. (2021). *Open-access collection of crystal structures of organic, inorganic, metal-organics compounds and minerals, excluding biopolymers*. http://www.crystallography.net/cod/

Nakamoto, K. (1986). *Infrared and Raman Spectra of Inorganic and Coordination Compounds*. Wiley.

Nilchi, A., Saberi, R., Moradi, M., Azizpour, H., & Zarghami, R. (2011). Adsorption of cesium on copper hexacyanoferrate–PAN composite ion exchanger from aqueous solution. *Chemical Engineering Journal, 172*(1), 572-580.

Parajuli, D., Takahashi, A., Noguchi, H., Kitajima, A., Tanaka, H., Takasaki, M., Yoshino, K., & Kawamoto, T. (2016). Comparative study of the factors associated with the application of metal hexacyanoferrates for environmental Cs decontamination. *Chemical Engineering Journal, 283*, 1322-1328.

Rahman, R. O. A., Ibrahium, H. A., & Hung, Y.-T. (2011). Liquid radioactive wastes treatment: A review. *Water, 3*(2), 551-565.

Shanker, U., Jassal, V., & Rani, M. (2017). Degradation of toxic PAHs in water and soil using potassium zinc hexacyanoferrate nanocubes. *Journal of Environmental Management, 204*, 337-348.

Singh, S., Eapen, S., Thorat, V., Kaushik, C. P., Raj, K., & D'Souza, S. F. (2008). Phytoremediation of ^{137}cesium and ^{90}strontium from solutions and low-level

nuclear waste by *Vetiveria zizanoides*. *Ecotoxicology and Environmental Safety*, *69*(2), 306-311.

Sun, S. D., Zhang, X. C., Cui, J., & Liang S. H. (2020). Identification of the Miller indices of a crystallographic plane: A tutorial and comprehensive review on fundamental theory, universal methods based on different case studies and matters needing attention. *RCS Nanoscale*, *12*(32), 16,657-16,677.

Takahashi, A., Kitajima, A., Parajuli, D., Hakuta, Y., Tanaka, H., Ohkoshi, S., & Kawamoto, T. (2016). Radioactive cesium removal from ash-washing solution with high pH and high K^+-concentration using potassium zinc hexacyanoferrate. *Chemical Engineering Research and Design*, *109*, 513-518.

Todd, T. A., Batcheller, T. A., Law, J. D., & Herbst, R. S. (2004). *Cesium and strontium separation technologies literature review*. United States. https://doi.org/10.2172/910643

Vincent, T., Vincent, C., & Guibal, E. (2015). Immobilization of metal hexacyanoferrate ion-exchangers for the synthesis of metal ion sorbents–A mini-review. *Molecules*, *20*(11), 20,582-20,613.

Vipin, A. K., Ling, S., & Fugetsu, B. (2014). Sodium cobalt hexacyanoferrate encapsulated in alginate vesicle with CNT for both cesium and strontium removal. *Carbohydrate Polymers*, *111*, 477-484.

Vipin, A. K., Ling, S., & Fugetsu, B. (2016). Removal of Cs^+ and Sr^{2+} from water using MWCNT reinforced Zeolite-A beads. *Microporous and Mesoporous Materials*, *224*, 84-88.

Wang, L., Feng, M., Liu, C., Zhao, Y., Li, S., Wang, H., Yan, L., Tian, G., & Li, S. (2009). Supporting of potassium copper hexacyanoferrate on porous activated carbon substrate for cesium separation. *Separation Science and Technology*, *44*(16), 4023-4035.

Williams, A. N., Pack, M., & Phongikaroon, S. (2015). Separation of strontium and cesium from ternary and quaternary lithium chloride-potassium chloride salts via melt crystallization. *Nuclear Engineering and Technology*, *47*(7), 867-874.

Xu, C., Wang, J., & Chen, J. (2012). Solvent extraction of strontium and cesium: A review of recent progress. *Solvent Extraction and Ion Exchange*, *30*(6), 623-650.

Yang, H., Sun, L., Zhai, J., Li, H., Zhao, Y., & Yu, H. (2014). In situ controllable synthesis of magnetic Prussian blue/graphene oxide nanocomposites for removal of radioactive cesium in water. *Journal of Materials Chemistry A*, *2*(2), 326-332.

Yasunari, T. J., Stohl, A., Hayano, R. S., Burkhart, J. F., Eckhardt, S., & Yasunari, T. (2011). Cesium-137 deposition and contamination of Japanese soils due to the Fukushima nuclear accident. *Proceedings of the National Academy of Sciences*, *108*(49), 19,530-19,534.

Zong, Y., Zhang, Y., Lin, X., Ye, D., Qiao, D., & Zeng, S. (2017). Correction: Facile synthesis of potassium copper ferrocyanide composite particles for selective cesium removal from wastewater in the batch and continuous processes. *RSC Advances*, *7*(54), 33,974-33,974.